TEXAS TECH UNIVERSITY
Libraries™

MAPPING FOREST AGE AND CHARACTERIZING VEGETATION STRUCTURE AND SPECIES COMPOSITION IN TROPICAL DRY FORESTS

Ecological Indicators 120 (2021) 106955

Contents lists available at ScienceDirect

Ecological Indicators

journal homepage: www.elsevier.com/locate/ecolind

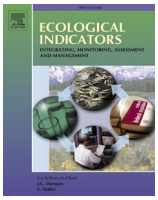

Mapping forest age and characterizing vegetation structure and species composition in tropical dry forests

G. Reyes-Palomeque [a], J.M. Dupuy [a], C.A. Portillo-Quintero [b], J.L. Andrade [a], F.J. Tun-Dzul [a], J. L. Hernández-Stefanoni [a,*]

[a] Centro de Investigación Científica de Yucatán A.C. Unidad de Recursos Naturales, Calle 43 # 130, Colonia Chuburná de Hidalgo, 97205 Mérida, Yucatán, Mexico
[b] Geospatial Technologies Laboratory, Department of Natural Resources Management, Texas Tech University, Box 42125, Lubbock, TX 79409-2125, United States

ARTICLE INFO

Keywords:
Stand age
Land cover classification
Secondary forest
Species richness and composition
Vegetation attributes
Chronosequence

ABSTRACT

Land use changes generate a mosaic of forest patches with different ages of abandonment (i.e. succession) intermingled with other land uses. Mapping the successional age of vegetation is crucial to understand carbon accumulation patterns and the recovery of vegetation structure, diversity, and composition of forests over time. The overall objective of this research was to produce maps portraying secondary vegetation age classes and to assess how successional age classes can be related to vegetation structure, diversity and composition in two types of tropical dry forests (TDF) in the Yucatan Peninsula. We used a two-stage image classification process. First, SPOT-5 imagery were segmented and then classified using a Random Forests method. Second, the classified images were post-processed to rectify any classification errors. Additionally, we evaluated the association between the different forest age classes and vegetation structure, species richness and composition using a separate Random Forests classification of field plot data. Post-processing improved the accuracy of the Random Forests classifications by 14.19% and 16.28% for the tropical semi-deciduous and semi-evergreen forests, to attain final accuracy values of 91% and 88.37%, respectively. Vegetation structure, richness and composition were all strongly associated with successional age, accounting for 77.7% and 84.7% of the total variation among forest age classes for the tropical semi-deciduous and semi-evergreen forests respectively. Therefore, the forest age maps obtained can be related to attributes of vegetation structure, diversity and composition that are useful for biodiversity conservation, forest management and climate change mitigation.

1. Introduction

Tropical dry forests (TDF) are the least protected yet most threatened terrestrial ecosystem in the tropics due to anthropic activities that cause widespread deforestation and forest degradation (Portillo-Quintero and Sanchez-Azofeifa, 2010; Portillo-Quintero et al., 2015; Coelho et al., 2016: Powers et al., 2018; Stan and Sanchez-Azofeifa, 2019). Moreover, TDF are affected by natural disturbances such as wildfires and extreme weather events such as hurricanes and long droughts (De la Barreda-Bautista et al., 2011; Balvanera et al., 2012). At the same time, these forests supply many products including raw materials for construction, food, medicines, etc., and they provide several environmental services such as climate regulation, and harbour many plant and animal species (Portillo-Quintero et al., 2015; Powers et al., 2018). The conversion of forested areas to agricultural/pasture lands or human settlements is one of the major processes affecting these forests as well as the second largest source of CO_2 emissions to the atmosphere (Le Quéré et al., 2015). Tropical dry forests are one of the ecosystems most extensively used by society, as they grow on fertile soils, are generally located in flat, low-elevation areas, and are easy to clear due to their simpler vegetation structure compared to their humid and wet counterparts (Portillo-Quintero et al., 2015; Powers et al., 2018). Forest cover change leads to biodiversity loss and the modification of the structure, functioning and dynamics of these ecosystems. Deforestation has also converted many TDF landscapes into mosaics of secondary vegetation growing from previously used and subsequently abandoned lands, remnants of primary forests, together with numerous areas dedicated to agriculture, livestock activities, and human settlements (De la Barreda-Bautista et al., 2011; Torres et al., 2012).

The largest extension of TDF in Mexico is located in the Yucatan Peninsula. These forests have been used for slash-and-burn agriculture by the Mayan people for over two millennia (González-Cruz et al.,

* Corresponding author.
E-mail address: jl_stefanoni@cicy.mx (J.L. Hernández-Stefanoni).

https://doi.org/10.1016/j.ecolind.2020.106955
Received 31 March 2020; Received in revised form 29 August 2020; Accepted 10 September 2020
Available online 24 September 2020

2015). Slash-and-burn agriculture, one of the oldest and most extensively used land-use practices in the tropics, involves clearing forest areas that are used for growing crops during two or three years, followed by abandonment for approximately 15 to 40 years. The fallow period allows the forest to regenerate through secondary succession. The vegetation structure, species richness and composition of these secondary forests differ from those of primary or mature forests (Dupuy et al., 2012; Stan and Sanchez-Azofeifa, 2019). Estimating and mapping vegetation age is therefore important for biodiversity conservation and management, land use planning and climate change mitigation. However, few accurate maps of vegetation age are currently available in the tropics (Garcia Millan and Sanchez-Azofeifa, 2018; Sun et al., 2019).

Analysing secondary forest succession is essential to understand carbon accumulation and the recovery of vegetation structure, species richness, and species composition of forests over time (Chazdon, 2014; Stan and Sanchez-Azofeifa, 2019). Secondary forests can provide key ecosystem services, however their capacity to provide those services varies with successional age (Chazdon, 2014; Poorter et al., 2016). Secondary forest succession is most commonly studied through the chronosequence or space for time substitution method, in which forest stands of different ages since abandonment are characterized and compared to infer successional dynamics, without having to monitor permanent plots for many decades. Forest age data can be obtained from local landowners and can be grouped into successional age classes to allow comparisons of vegetation structure and composition among different studies (Arroyo-Mora et al., 2005; Cao et al., 2015; Martínez-Ramos et al., 2018). Having information about the distribution of forest age categories at landscape or regional scales helps formulating policies and strategies for forest conservation, restoration, and/or sustainable forest management (Stan and Sanchez-Azofeifa, 2019). However, chronosequences can only provide information for a limited number of forest stands within a landscape.

On the other hand, remote sensing provides spatially continuous data at regular time intervals and it is one of the most widely used tools for monitoring vegetation and its spatial and temporal dynamics (Lillesand et al., 2004). Numerous studies have sought to estimate the age of tropical forests using satellite imagery. Some studies have used time series of satellite imagery to evaluate changes in forest fragments over the course of several years (Helmer et al., 2010; Fujiki et al., 2016; Chazdon et al., 2016; Sun et al., 2019), whereas others have used classification algorithms for analysing the spectral data from satellite images acquired in a single year (Fiorella and Ripple, 1995; Lucas et al., 2000; Vieira et al., 2003). Both types of studies use field information to validate the obtained forest age maps (Vieira et al., 2003; Baccini et al., 2012; Frate et al., 2015; Song et al., 2015; Chazdon et al., 2016; Carreiras et al., 2017). Although both methods produce adequate classifications of forest age, the approach based on time series of satellite imagery generally uses medium spatial resolution imagery and only rarely uses high spatial resolutions; in addition, this method is generally restricted to no more than 30 years since land abandonment, given the availability of time series of satellite imagery. On the other hand, chronosequences use field information about the age of the forest stands to produce forest age maps in a single year without the need to use time series of field data, which are difficult to obtain (Carreiras et al., 2014, 2017).

Various machine-learning techniques have been used in recent years to produce categorical vegetation maps from multispectral imagery, including clustering algorithms such as decision trees and Random Forests (Breiman, 2001; Karlson et al., 2015). Other approaches include satellite-image segmentation techniques, known as object-based classification, which have shown to be a suitable alternative to traditional per-pixel classification methods. Although segmentation techniques can be used with images of different spatial resolutions (Dorren et al., 2003; Lobo et al., 1996), they seem to be more helpful when applied to high-resolution imagery. This is because these methods make a partition of the image into homogeneous areas based on their spectral information. Segmentation methods have the additional advantage of using ancillary information such as the size, shape or texture of the image elements only visible in high resolution imagery (Dorren et al., 2003; Im et al., 2008).

This study sought to map forest age classes of two types of secondary TDF in the Yucatan Peninsula (semi-deciduous and semi-evergreen) and to evaluate the relationship between age classes and secondary forest structure, species diversity and composition in each forest type in order to assess which vegetation attributes are most strongly associated with forest age classes. We propose a method to improve the accuracy of mapping the spatial distribution of forest age classes based on a classification of spatial segments with similar spectral features created from high-resolution imagery and a post-processing procedure. Finally, we assess relationships between forest age classes and attributes of vegetation structure, diversity and composition in each forest landscape to allow interpreting forest age maps in terms of vegetation attributes that are critical for biodiversity conservation, forest management, and climate change mitigation.

2. Data and methods

2.1. Study area

The study area is located in the Yucatan Peninsula and encompasses two TDF landscapes (Fig. 1). The first landscape, named Kaxil Kiuic (hereafter KK), is located in the southwest part of the state of Yucatán, Mexico. This site comprises a total area of about 352 km^2 (22 × 16 km), including flat areas and low hills 60 to 190 m above sea level, and is covered by semi-deciduous tropical forest. The climate is warm humid, with summer rains and a pronounced dry season from November to April or May; mean annual temperature is 26 °C and average annual rainfall ranges between 1,000 and 1,200 mm (Flores and Espejel, 1994). This landscape is dominated by secondary vegetation of different ages since abandonment after being used for slash-and-burn agriculture. Vegetation canopy is approximately 8 to 13 m tall. The most abundant tree species in this landscape include *Neomillspaughia emarginata* (H. Gross) S.F. Blake, and *Gymnopodium floribundum* Rolfe. (Polygonaceae), *Lonchocarpus xuul* Lundell, *Mimosa bahamensis* Benth. and *Caesalpinia gaumeri* Greenm, (Fabaceae) and *Bursera simaruba* (L.) Sarg. (Burseraceae), among others (Hernández-Stefanoni et al., 2011; Miranda-Plaza, 2014).

The second landscape, named José María Morelos (hereafter JMM), is located in the southern part of the State of Quintana Roo, Mexico. This site has a total area of 351 km^2 (19.5 × 18 km) and is covered by semi-evergreen tropical forest and some areas of seasonally flooded low-stature tropical forest. The climate is warm subhumid, with a dry season from December to April and a rainy season from May to November; mean annual temperature is 26 °C and mean annual rainfall ranges between 1,100 and 1,400 mm (Flores and Espejel, 1994). This landscape includes areas in various stages of secondary succession after being used for slash-and-burn agriculture and cattle pasture (Miranda-Plaza, 2014; Hernández-Stefanoni et al., 2014). The forest canopy is approximately 15 to 25 m tall, and the most abundant tree species include *Manilkara zapota* (L.) P. Royen (Sapotaceae), *Piscidia piscipula* (L.) Sarg. and *Lonchocarpus rugosus* Benth. (Fabaceae), *Bursera simaruba* (L.) Sarg. and *Guettarda combsii* Urb. (Rubiaceae), among others (Hernández-Stefanoni et al., 2011; Miranda-Plaza, 2014).

2.2. Field data collection and calculation of vegetation attributes

Field data were obtained during the rainy seasons of 2008 and 2009. A total of 276 sampling units were located in Kaxil Kiuic, whereas 86 sampling units were situated in José María Morelos (Fig. 2). The sampling plots were allocated seeking to cover the whole range of forest ages and environmental conditions present in each landscape. In both landscapes, the sampling units consisted of a 200 m^2 circular plot with a nested 50 m^2 concentric circular plot. In the 200 m^2 plots, all woody

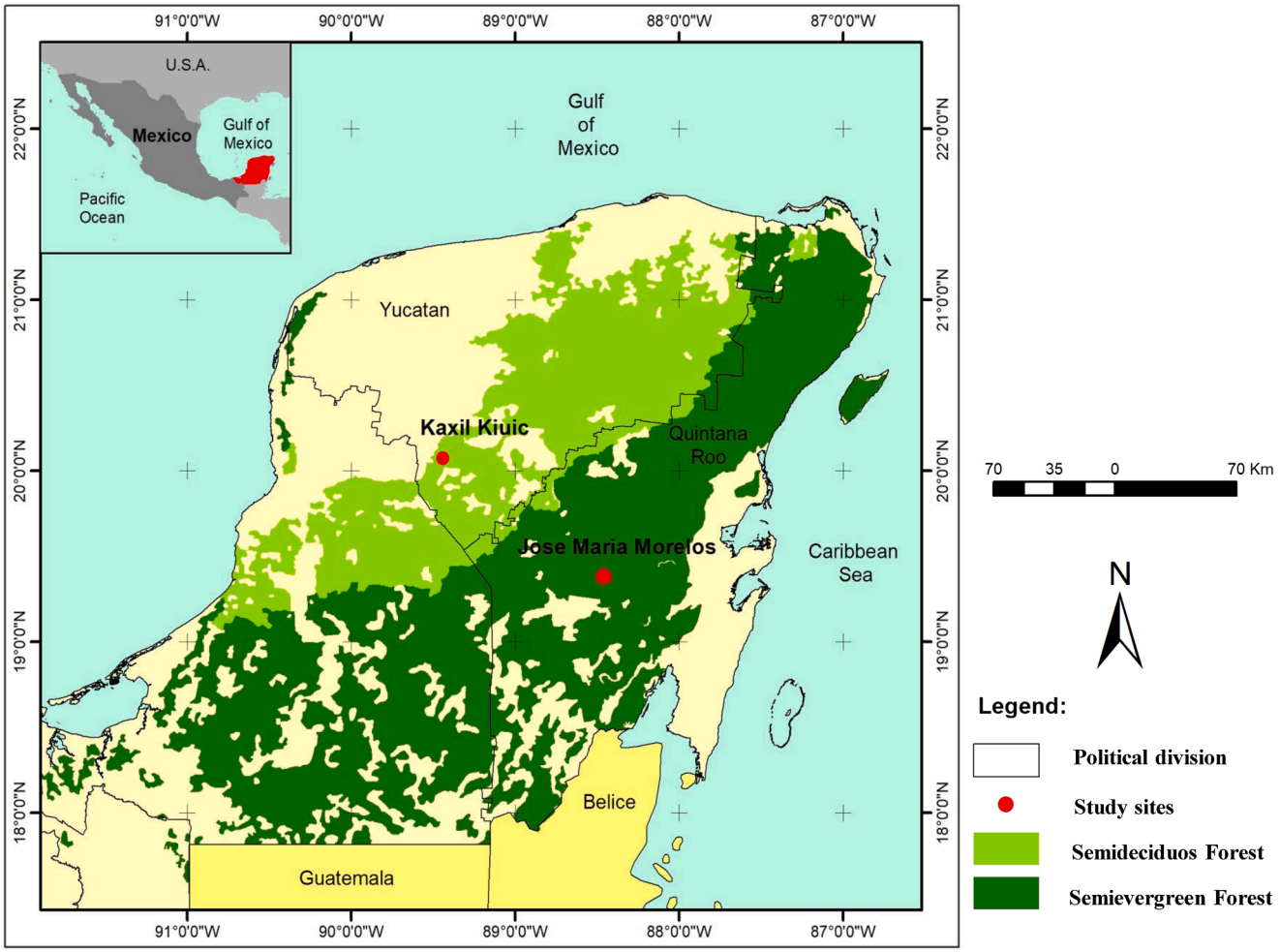

Fig. 1. Location of the study sites in the Yucatan Peninsula showing the two study sites in the forest of the Yucatan peninsula.

plants with a diameter at breast height (DBH) more than 5 cm, and in the 50 m^2 plot, all the individuals with DBH between 1 and 5 cm, were identified and measured. Individual plant attributes recorded include height (m), DBH (cm –measured at 1.3 m above the ground), and species name. The successional age of each sampling unit was determined based on interviews with local inhabitants or landowners.

Sampling units were classified into four forest age classes (class 1: 3–8 years; class 2: 9–16 years, class 3: 17–50 years; class 4: >50 years) for comparison with other studies in tropical forests (Fig. 2). The selection of the different age categories was based on the fact that some tropical forest plant attributes, such as biomass, basal area and species richness saturate with stand age, showing high rates of increase during the first 15 to 20 years, followed by much slower rates at older stand ages (Poorter et al., 2016, Marin-Spiotta et al., 2007). For each age class, the following vegetation structure attributes were estimated: basal area ($m^2 \cdot ha^{-1}$), abundance, mean DBH (cm), mean tree height (m), mean height of the ten tallest trees (m), and mean aboveground biomass ($Mg \cdot ha^{-1}$).

We used local and regional allometric equations to estimate aboveground biomass for each sampling unit in both landscapes. The equations take into consideration the vegetation type as well as DBH, height, wood density of trees, and growth form (trees, palms, and lianas) and were developed by Frangi and Lugo (1985), Chave et al. (2003), Chave et al. (2005), Guyot (2011), and Ramírez et al. (2019), see Table S1. Wood density values for most of the tree species were obtained from local studies, others were obtained from the literature (Brown, 1997; Aguilar-Rodríguez et al., 2001; Reyes-García et al., 2012; Sanaphre-Villanueva et al., 2016). Species richness was determined for each sampling plot and successional age class.

2.3. Remotely sensed data and image processing

For this study, we used SPOT-5 multispectral imagery. The scenes were acquired in January 2005 and January 2010 for KK and JMM, respectively. SPOT-5 imagery has a spatial resolution of 10 m per pixel in four spectral bands: green band (b1), 0.5–0.59 μm; red band (b2), 0.61–0.68 μm; near-infrared band (b3), 0.78–0.89 μm; and the shortwave infrared band (b4), 1.58–1.75 μm.

First, we created objects (segments) from the SPOT 5 imagery in both landscapes using an image segmentation procedure. This procedure consisted in joining neighbouring pixels sharing similar spectral features, aiming to properly represent areas with vegetation clustered into different forest age groups and other cover areas. The segmentation process was carried out using the RSGISLib package from Python 3.6 software (van Rossum, 1995). Through the segmentation process, images were partitioned into objects with homogeneous spectral characteristics, which corresponded to roads, agricultural areas, water bodies, and vegetation areas in different successional stages.

In a second stage, image objects instead of pixels were used in an automated Random Forest classification algorithm for mapping forest age classes. We used 50% of field sampling plots, as training sites (138 and 43 plots respectively for KK and JMM landscapes), while the remaining 50% of plots were used to validate the classification. These sampling-units were randomly chosen within each forest age class using

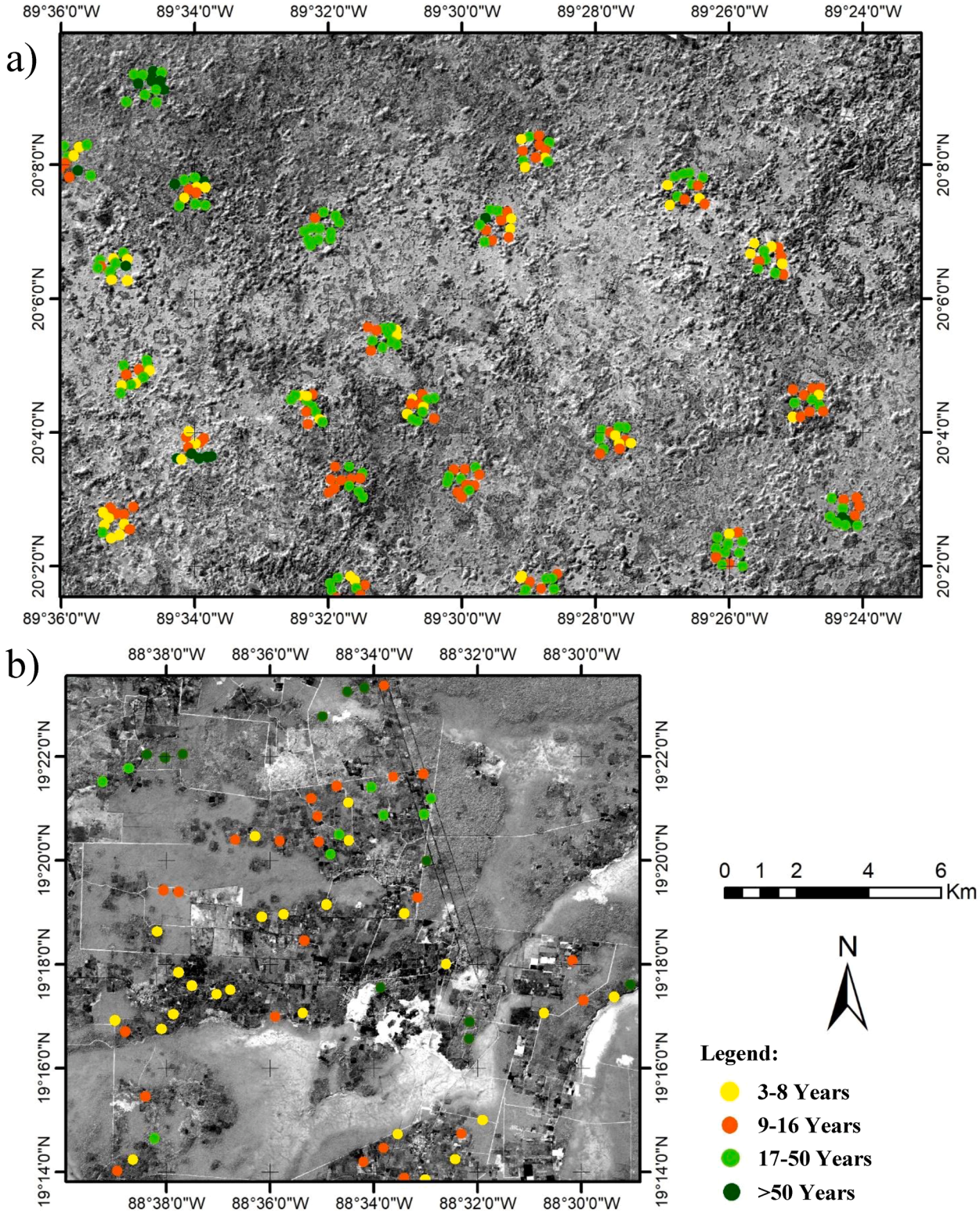

Fig. 2. Location of sampling plots in the Kaxil Kiuc (a) and José María Morelos (b) landscapes classified by forest age class.

the software QGIS 3.6 (QGIS Development Team, 2017). The sample selection preserved the age ranges observed in the field (Fig. 2). The segments in which 50% of the field plots fell were considered as training sites. Subsequently, we calculated zonal statistics (mean, median, and standard deviation) for each training site and we used these data for examining the spectral separability of forest age classes.

The training sites (segments) were used to apply the Random Forest classification algorithm using the randomForest package (RColorBrewer and Liaw, 2018) in R (R Development Core Team, 2017). As a result, the algorithm predicted the spatial distribution of the different land cover classes including vegetation in the four successional age classes. Random Forest is a non-parametric algorithm considered as one of the most robust classifiers; it can be used with large datasets and reduces the data overfitting issue, which can occur when the samples are not fully

representative (Breiman, 2001; Cutler et al., 2012). The random forest model provides an importance ranking predictor (the mean decrease in accuracy), which evaluates the change in the accuracy if one of the variables is left out of the model.

In a third stage, land cover classes obtained from the automated classification algorithm were subjected to post-processing in order to improve the accuracy of the forest age maps. This process consists of reclassifying those forest age-class polygons showing spectral confusion. To this end, an in-depth visual inspection of all segments was carried out to rectify potential errors, using zonal statistics of training sites. The reclassification was made by comparing segment values versus those of field training sites.

Finally, the two land-cover maps, i.e., the one obtained directly with the Random Forest algorithm and the one obtained after post-processing, were validated using the remaining 50% of the field-sampling plots that were not used to create the training sites. The accuracy of both maps and that of each forest age class were assessed using a confusion matrix, that is, a table that measures the agreement between classes in the map and classes on the ground (Campbell and Wynne, 2011). The overall accuracy of the classified forest age map was calculated by dividing the total number of correctly classified plots of the forest age map, over the total number of reference sample plots. The producer accuracy was then calculated as the number of correctly classified plots of the forest age map over the number of reference sample plots in the same class and it indicates the proportion of plots on the ground for each age class that were correctly classified on the map. The user accuracy is the proportion of plots in a particular age category on reference sample class data that is also mapped as that age category. This index measures the proportion of plots in a forest age class that will be present on the map (Campbell and Wynne, 2011).

2.4. Data analyses

To assess the relationships between the forest age classes and vegetation structure, species richness and species composition, a second Random Forest classification was carried out using the Model Map package (Freeman et al., 2018) for R (R Development Core Team, 2017). This classification was not spatially explicit, meaning it was carried out using field data exclusively and not satellite imagery data. For this classification, 70% of the field-sampling plots (193 and 60 plots respectively for KK and JMM landscapes) were used for training the model and the remaining 30% (83 and 16 plots respectively for KK and JMM landscapes) were used to validate the classification. Additionally, Moran's I test was applied to test for spatial autocorrelation in the vegetation structure variables. The vegetation predictor variables were ranked by their mean decrease in accuracy to assess their relative contribution to distinguish among forest age classes.

To assess differences in vegetation structure and species composition among forest age classes, the average and the 95% confidence intervals of vegetation attributes (diameter, stature, abundance, basal area, species richness and species composition) in each forest age class were calculated separately for the two types of TDF.

An exploratory analysis of species composition among forest age classes in each landscape was carried out using Non-metric Multidimentional Scaling (NMDS) with the Vegan package (Oksanen et al., 2007) for R (R Development Core Team, 2017). The NDMS is a non-parametric ordination technique that projects the multidimensional species-by-plot data matrix onto a lower-dimensional space, in this case we obtained three ordination axes. To explore and visually represent differences in species composition among forest age classes, the sample sites were colour coded by age class and the centroid of each age class was indicated in the NDMS ordination plots. In addition, to test for significant differences in species composition between the forest age classes, we employed PERMANOVA analysis, a nonparametric analogue of multivariate analysis of variance that tests variability within and between groups, but is free of parametric assumptions of multivariate normality and homogeneity of variances. The PERMANOVA analysis was carried out using a matrix of species abundance and forest age classes as a categorical explanatory variable with the Vegan package (Oksanen et al., 2007) for R (R Development Core Team, 2017).

Finally, the most important species in each forest age class were identified and the Simpson dominance index (D) was calculated to examine how species dominance varied among successional age classes in each landscape. This index is strongly influenced by the most abundant species and is less sensitive to species richness (Magurran, 2004).

3. Results

A classified map of forest age classes after performing both the random forest classification method and the post-processing of the SPOT 5 imagery for the KK and JMM landscapes yielded an overall accuracy of 91% and 88.37% (Fig. 3, Table 1), respectively. Compared to the map obtained from the random forest classification alone, the post-processing procedure improved the accuracy of the forest age map by 14.19% and 16.28% respectively for KK and FCP (Supplementary Fig. 1 and Table S2).

The age class with the highest user accuracy, after applying both the random forest classification method and the post-processing, was the 17–50 yr. class (95.3% accuracy) in the KK landscape (Table 1) and the 9–16 yr. class (90.9% accuracy) in the JMM landscape (Table 1). The lowest user accuracy was found in the > 50 yr. class in the KK landscape and the 17–50 yr class in the JMM landscape, with an 80% accuracy in both cases (Table 1).

The highest producer accuracy was observed in the 9–16 yr. class (95.2% accuracy) in the KK landscape, and in the 9–16 and > 50 yr. classes (100% accuracy in both cases) in the JMM landscape. The lowest producer accuracy was recorded in the > 50 yr. class in KK and in the 17–50 yr. class in JMM (80% in both cases; Table 1). The user and producer accuracies have similar values in all forest age classes for KK landscape. However, the fact that there is a higher value of user accuracy than producer accuracy for the forest with more than 50 years in JMM landscape (a difference 16.7%) indicates that this class had the highest magnitude of misclassification compared to the others classes.

The land-cover classes with the highest coverage were the 17–50 yr. class in the KK landscape (39.50%) and the >50 yr. class in the JMM landscape (36.8%), respectively, followed by the >50 yr. class (28.4%), and the 17–50 yr. (34.6%), respectively for KK and JMM landscapes. (Table 2).

The most important variables for mapping forest age classes based on the random forest classification method with satellite images were the mean and standard deviation of the red (b2) and near-infrared (b3) bands from SPOT imagery for the KK site, while the most important variables for JMM, were the mean and standard deviation of the green band (b1), the median of the near-infrared (b3) and the mean of the red (b2) bands of SPOT 5 imagery (Fig. 4).

The second Random Forest classification algorithm carried out to evaluate relationships between forest age classes and vegetation attributes revealed that vegetation attributes accounted for 77.7% and 84.7% of the variation among forest age classes in the KK and JMM landscapes, respectively. The most important variables, to characterize forest age classes from vegetation attributes, were basal area (BA), diameter at breast height (DBH), mean height of the 10 tallest trees, mean tree height and aboveground biomass (AGB) for the KK landscape. In JJM, the vegetation attributes that best distinguished among forest ages classes were mean height of the 10 tallest trees, basal area (BA), sample plot scores on ordination axis 1 from NMDS, aboveground biomass (AGB) and diameter at breast height (DBH) (Fig. 5). We found no significant spatial autocorrelation ($p > 0.05$) for any of the vegetation attributes in either landscape.

The forest age classes in the KK landscape clearly differed in vegetation structure, especially in basal area, diameter, height of the ten tallest trees, mean tree height, and aboveground biomass (Fig. 6). In the

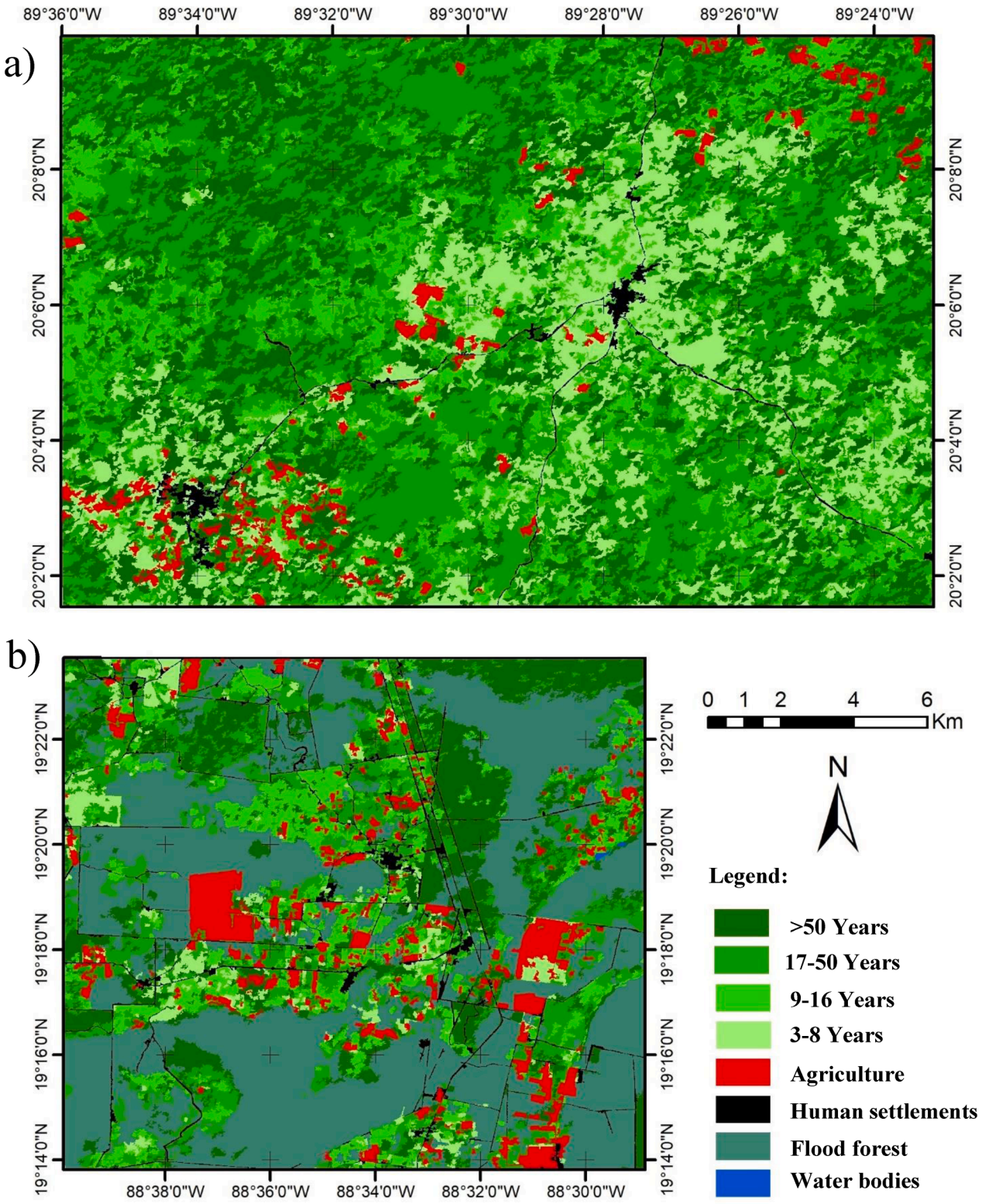

Fig. 3. Forest age map of the tropical dry forests in the Kaxil Kiuc (a) and José María Morelos (b) landscapes obtained after a classification with random forest of SPOT 5 imagery and post-processing.

JMM landscape, the forest age classes differed in terms of both vegetation structure and composition, especially in mean height of the 10 tallest trees, basal area (BA), aboveground biomass (Fig. 6) and plot scores on ordination axis 1 from NMDS (Fig. 7). In both landscapes, in addition to showing significant differences between forest age classes, most variables increased with time since abandonment, except for abundance, which decreased.

A total of 204 woody plant species in 52 families were recorded in the KK landscape, whereas 223 woody plant species in 50 families were recorded in the JMM landscape. The plant species with the highest importance value (IVI) in each forest age class are shown in Table 3.

Exploratory NMDS ordination analyses revealed that species

Table 1
Validation of the age map for tropical dry forests of the Kaxil Kiuic and José María Morelos landscapes after using Random Forest classification and post-processing.

Landscape Age class (Years)	Producer accuracy (%)	User accuracy (%)	Overall accuracy (%)
Kaxil Kiuic			91.0
3–8	85.0	89.5	
9–16	90.9	95.2	
17–50	95.3	91.0	
+50	80.0	80.0	
José María Morelos			88.4
3–8	90.0	92.3	
9–16	90.9	100.0	
17–50	80.0	80.0	
+50	83.3	100.0	

Table 2
Percent coverage of forest age classes in the Kaxil Kiuic and José María Morelos landscapes.

	Kaxil Kiuic		José María Morelos	
Forest Age Classes	Surface (ha)	(% of Coverage)	Surface (ha)	(% of Coverage)
>50 Years	10,021.3	28.4	6,033.6	36.8
17–50 Years	13,930.2	39.5	5,670.8	34.6
9–16 Years	5,476.6	15.5	3,426.8	20.9
3–8 Years	5,874.4	16.6	1,246.7	7.6
TOTAL	35,302.3	100.0	16,377.9	100.0

composition differed among the forest age classes in both landscapes, especially in JMM (Supplementary Fig. 2). The PERMANOVA tests confirmed that these differences were significant ($P < 0.001$), although they accounted for a small proportion of the total variation in species composition ($R^2 = 0.09$ in Kaxil Kiuic and $R^2 = 0.22$ and José María Morelos, respectively (Table 4).

The two landscapes studied showed contrasting patterns of species dominance (Simpson's index). In KK, the highest dominance (0.12) was found in the early successional class (3–8 yr.), whereas in JMM, the highest dominance (0.11) corresponded to old-growth forests (>50 yr.) (Table 5).

4. Discussion

4.1. Tropical dry forest age maps

The methodology used in this study allowed us to obtain accurate forest age maps for the semi-deciduous and semi-evergreen tropical forests (overall accuracy = 91.0% and 88.4%, respectively). These overall accuracy values are higher than those reported in previous studies of tropical forests (80–88% accuracy) (Helmer et al., 2010, Pasher and King, 2011, Fujiki et al., 2016, Carreiras et al., 2017, Sun et al. 2019). Most recent studies on vegetation classification, either in general or differentiating forest age areas, have combined spectral information from satellite images with image texture information and environmental or topographic data (Berberoglu et al., 2000; Gallardo-Cruz et al., 2012; Carreiras et al., 2017). Although this approach could enhance the accuracy of our classifications, we were able to produce highly accurate maps of forest coverage in different successional age classes using exclusively the reflectance in the different SPOT-5 bands with the Random Forest classification algorithm, a thorough post-processing process and chronosequence data. In particular, the use of high-resolution imagery allowed us to better detect variability in the different vegetation elements, water bodies or agricultural areas, compared to medium-resolution imagery (Liu and Xia, 2010). Moreover, the segmentation (object-based classification) of the images allowed a better spectral separation of different successional stages (Nelson et al., 2000). However, segmentation can also produce a lower precision when segments do not adequately represent the objects on the surface, particularly in forested areas where pixels include a mix of both forest canopy and gaps (Pasher and King, 2011).

An important methodological step in this study was the post-processing of the images that were first classified using segments with a Random Forest algorithm. This step increased the accuracy of the vegetation cover maps of different successional age classes by 14.19% and 16.28%, for the KK and JMM landscapes, respectively. Clearly, post-processing played a central role in improving the accuracy of

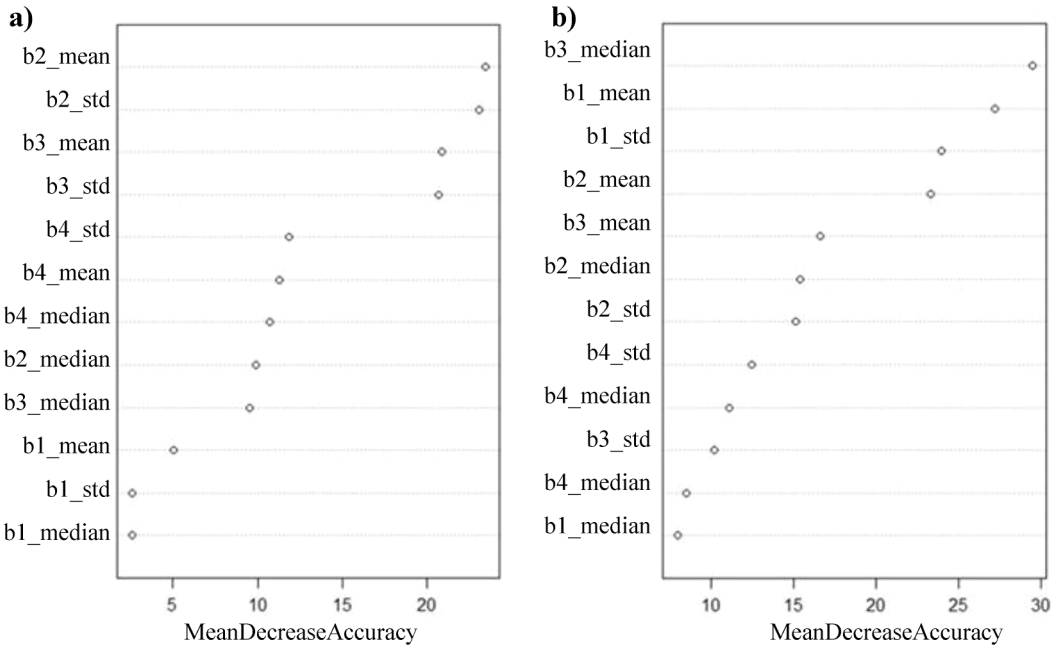

Fig. 4. Random forest predictor importance ranking (mean decrease in accuracy) using SPOT 5 imagery predictor variables in Kaxil Kiuic (a) and José María Morelos (b). b1 = green band; b2 = red band; b3 = shortwave infrared band and b4 = near-infrared band of Spot 5 Imagery; mean; median; std = standard deviation.

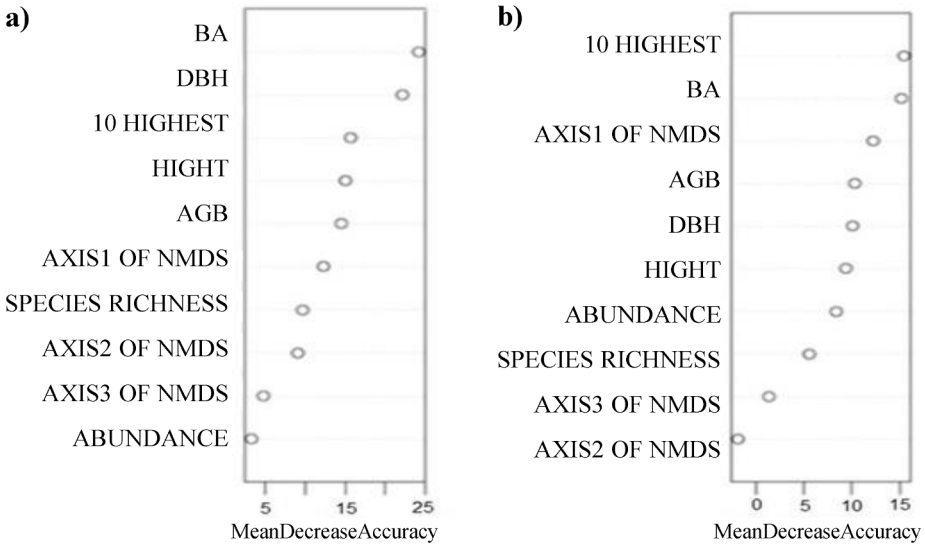

Fig. 5. Random forest predictor importance ranking (mean decrease in accuracy) using vegetation attributes as predictor variables in Kaxil Kiuc (a) and José María Morelos (b). BA = basal area; DBH = diameter at breast height; 10 HIGHEST = Mean height of the 10 tallest trees; AGB = aboveground biomass; NMDS = Non-metric Multidimensional Scaling.

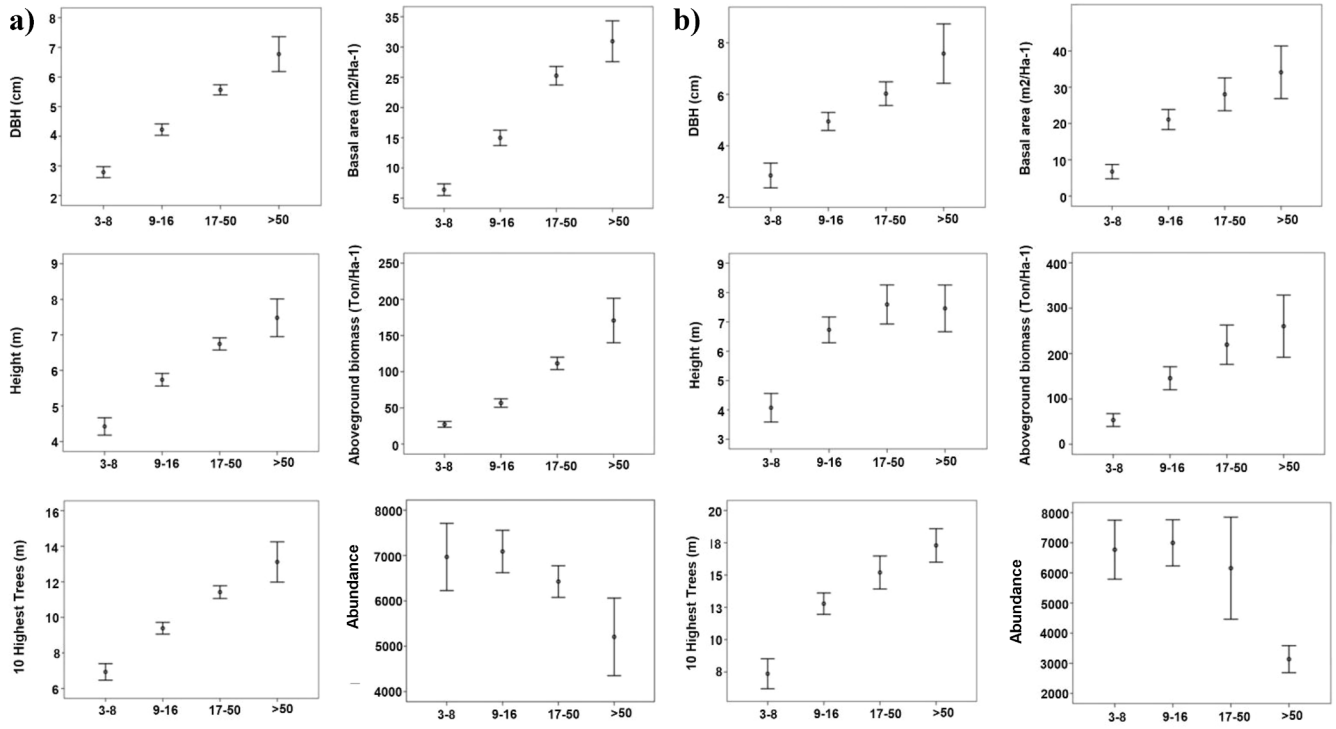

Fig. 6. Mean values and 95% confidence intervals of vegetation structure variables in each forest age class in Kaxil Kiuc (a) and José Maria Morelos (b). DBH = diameter at breast height, Height = mean tree height, 10 Highest Trees = Mean height of the 10 tallest trees.

classification of forest age classes in both landscapes. This was achieved through a combination of information from the training sites, zonal statistics calculated for the entire area and visual examination, which allowed us to separate areas of different successional age classes. For example, the spectral information obtained from satellite images on the early successional classes may be confounded with that from areas of low or sparse vegetation (leading to a low initial classification accuracy). However, spectral information of early ages can easily be differentiated with a visual examination during post-processing (compare the values of producer accuracy for these classes in Tables S2 and Table 1). Similarly, fast recovery of vegetation structure attributes during secondary succession may cause intermediate-aged (17–50 yr.) forests to attain similar vegetation structure values compared to old-growth (>50 yr.) forests, and hence to show similar reflectance values in the different bands of multispectral images, as seems to have been the case in the JMM landscape (Fig. 6b).

The greater area of young forest age classes and lower percentage of mature forest cover in KK landscape compared to JMM landscape (Table 2) reflect differences in land-use practices. In KK, slash-and-burn agriculture has been the dominant land use for several centuries and the fallow period has been shortened, leading to a predominance of young secondary vegetation. On the other hand, in JJM, cattle pastures are

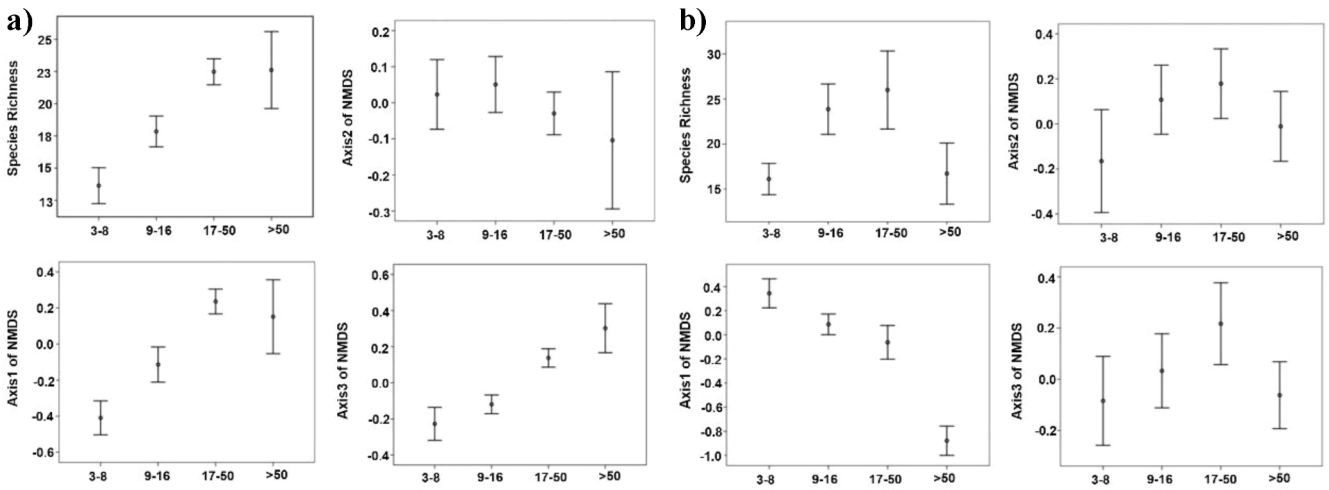

Fig. 7. Mean values and 95% confidence intervals of species richness and composition in each forest age class in Kaxil Kiuc (a) and José Maria Morelos (b).

Table 3
List of the most abundant species in each forest age class in the Kaxil Kiuic and José María Morelos landscapes.

3–8 Years	9–16 Years	17–50 Years	>50 Years
Kaxil Kiuic			
Neomillspaughia emarginata	*Neomillspaughia emarginata*	*Bursera simaruba*	*Caesalpinia gaumeri*
Mimosa bahamensis	*Bursera simaruba*	*Gymnopodium floribundum*	*Bursera simaruba*
Caesalpinia gaumeri	*Lysiloma latisiliquum*	*Lysiloma latisiliquum*	*Gymnopodium floribundum*
Piscidia piscipula	*Gymnopodium floribundum*	*Lonchocarpus xuul*	*Lonchocarpus xuul*
Bursera simaruba	*Mimosa bahamensis*	*Piscidia piscipula*	*Piscidia piscipula*
Lysiloma latisiliquum	*Piscidia piscipula*	*Thouinia paucidentata*	*Lysiloma latisiliquum*
Gymnopodium floribundum	*Lonchocarpus xuul*	*Neomillspaughia emarginata*	*Diospyros anisandra*
José María Morelos			
Piscidia piscipula	*Piscidia piscipula*	*Bursera simaruba*	*Brosimum alicastrum*
Lonchocarpus xuul	*Croton glabellus*	*Lysiloma latisiliquum*	*Pouteria reticulata*
Croton glabellus	*Bursera simaruba*	*Croton glabellus*	*Trichilia minutiflora*
Spondias radlkoferi	*Lysiloma latisiliquum*	*Piscidia piscipula*	*Piper amalago*
Sabal gretheriae	*Guettarda combsii*	*Coccoloba spicata*	*Manilkara zapota*
Lonchocarpus rugosus	*Allophylus cominia*	*Guettarda combsii*	*Pouteria campechiana*
Hamelia patens	*Sabal gretheriae*	*Dendropanax arboreus*	*Dalbergia glabra*

Table 4
PERMANOVA analyses of differences in species composition among forest age classes in the two landscapes studied.

Landscape		df	Sum of Squares	Mean Square	F	R^2	Pr (>F)
Kaxil Kiuic	Age	3	7.18	2.39	9.26	0.09	0.001
	Residual	272	70.27	0.25		0.90	
	Total	275	77.45			1.00	
José María Morelos	Age	3	4.98	1.65	5.95	0.22	0.001
	Residual	63	17.56	0.27		0.77	
	Total	66	22.55			1.00	

common and are generally maintained for decades, while slash-and-burn agriculture is less dominant and there is also selective timber extraction resulting in larger areas of mature forest (Chazdon, 2003). It

Table 5
Simpson's species dominance index in each forest age class in the two landscapes studied.

Landscape	(3–8 Years)	(9–16 Years)	(17–50 Years)	(>50 Years)
Kaxil Kiuic	0.12	0.06	0.04	0.05
José María Morelos	0.05	0.03	0.06	0.11

is worth noting that, in both landscapes, the oldest age class had comparatively low classification precision (producer accuracy in Table 1). Old-growth forests are characterized by having a complex and heterogeneous structure ranging from tall, dense, closed canopy conditions to more open conditions with short vegetation in canopy gaps (Chazdon, 2014), making them hard to classify, especially using high resolution imagery. On the other hand, we found comparatively low classification precision (producer accuracy) for the youngest forest age class in the KK landscape, but not in the JMM one (Table 1, S2). This may be due to differences in the predominant land-use practice in each landscape. The dominant land use (in terms of land cover) in JMM is cattle pastures, in which large areas (10 – 200 ha) are uniformly covered with short grasses with no remnant trees for several decades. In contrast, the dominant land use in KK is traditional slash-and-burn agriculture, which occupies smaller areas (1 – 4 ha) for a much shorter period (2–4 years) and are covered by corn, squash, beans and other crops (González-Cruz et al., 2015). Thus, the contrast between agricultural lands and early successional forests is likely much greater (allowing a better classification of these forests) in JMM than in KK. This suggests that the predominant land-use practice may influence the accuracy with which early successional forests can be classified.

Finally, many studies mapping forest age consider as an alternative to the use of time series data for detecting age classes is the use of chronosequences, that is, field plots of different successional age or time since abandonment (Vieira et al., 2003; Fujiki et al., 2016; Carreiras et al., 2017). In our study, we established successional age from interviews with local land-owners, villagers and farmers. This is important when using classification algorithms such as Random Forest, since a fraction of the field data can be used for training the model and the remaining portion is used for validating the forest age maps obtained.

4.2. Vegetation structure, species richness and species composition in forest age classes

An important goal of this study was to assess relationships between forest age classes and vegetation structure, species diversity and

composition. In this way, the forest age maps obtained could be interpreted in ecological terms and used for guiding forest management and conservation strategies and land-use practices. We found that vegetation attributes are strongly associated with variation among forest age classes (accounting for 77.7% and 84.7% of the variation in KK and JMM respectively), as reported elsewhere (Eaton and Lawrence, 2009). In both study landscapes, vegetation attributes such as basal area, mean tree height, aboveground biomass, and diameter increased with successional age and differed among forest age classes. Some studies have shown that vegetation attributes such as aboveground biomass, species richness and tree size are strongly and positively related to forest successional age (Zhang and Chen, 2015). These results are similar to those from other studies conducted in the same study area (Dupuy et al., 2012; Miranda-Plaza, 2014).

In the KK landscape, the five vegetation attributes that contribute most to differentiate among forest age classes were all structural attributes (Fig. 5 a). In this landscape, the early successional classes typically display a large number of small individuals, resulting in distinctively lower values of basal area, diameter, and height, compared to more advanced successional stages. Other studies have reported that a high density of small individuals during the early successional stages can be produced by germination processes (Ruiz et al., 2005) coupled with colonization or establishment of species through dispersal or regrowth (Maza-Villalobos et al., 2011). The relatively lower contribution of species richness and composition to distinguish among forest age classes in this landscape seems to be associated with the large variation in these vegetation attributes shown by the old-growth (>50 yr.) forests (Fig. 6a, Fig. 7a). This large variation likely reflects the effect of topography, since this area is characterized by the presence of low hills with distinct soil conditions and mostly old-growth forests, alternating with flat areas (Dupuy et al., 2012). Indeed, the latter study found significant differences in soil conditions as well as in forest structure, diversity and composition between hills and flat areas.

In the JMM landscape, forest canopy height (height of the tallest trees), basal area and species composition (sites scores on NMDS axis 1) were the most important vegetation attributes for differentiating forest age classes. The semi-evergreen tropical forest in this landscape has different topographic (flat areas) and soil conditions and higher precipitation (and water availability) than the semi-deciduous tropical forest of the KK landscape. Therefore, trees in the semi-evergreen forest are able to attain larger sizes (in terms of basal area, aboveground biomass, and tree height) and at earlier successional ages compared to the semi-deciduous forest (Fig. 6). On the other hand, selective logging practiced almost exclusively in the JMM landscape (Avella et al., 2019; López-Jiménez et al., 2019) involves the extraction of the biggest trees, thereby reducing mean tree height, basal area and above ground biomass of old-growth forests. This could help explain the similar values of these structural parameters shown by advanced (17–50 yr) and old-growth (>50 yr) forests in JJM (Fig. 6b).

Selective logging could also help explain the different patterns of species richness and dominance between the two forest landscapes studied. Surprisingly, old growth forests in JMM showed lower species richness than intermediate (9–16 yr) and advanced (17–50 yr) forests as well as the highest species dominance (Table 5). Overexploitation (leading to local extirpation) of several valuable timber species in old-growth forests in this landscape could be partly responsible for these unexpected patterns. These forests showed high dominance by a few slow-growing late-successional species that are valued for food and/or chewing gum, such as *Brosimum alicastrum*, *Pouteria recticulata* and *Manilkara zapota*, and which are known to have been favoured by ancient Mayan peasants over several centuries (White and Hood, 2004). Strong dominance by a few favoured species in the old-growth forests can also explain the humped shape pattern of species richness with successional age found in JMM (Fig. 7b) which is in agreement with the intermediate disturbance hypothesis (Connell, 1978). In contrast, in the KK landscape, the strongest dominance was found in the youngest (3–8 yr.-old) forests, which were dominated by a few very abundant pioneer species such as *Neomillspaughia emarginata*, *Mimosa bahamensis*, and *Caesalpinia gaumeri*. This latter result is in line with successional theory and empirical findings in tropical forests in general (Chazdon, 2014).

We found minor (although significant) differences in species composition between forest age classes. For example, in KK we found many species that are common in different age classes, such as *Neomillspaughia emarginata*, *Bursera simaruba*, *Gymnopodium floribundum*, *Caesalpinia gaumeri*, *Lonchocarpus xuul*, and *Piscidia piscipula* (Table 3). This is consistent with previous findings in the Yucatan Peninsula that different forest age classes share many dominant species (López-Jiménez et al., 2019; Sanaphre-Villanueva et al., 2017; Dupuy et al., 2012). This dominance of generalist species across secondary forest succession may be partly the result of a long history of land use, mainly for slash and burn agriculture, and forest management by the Mayan people (Sanaphre-Villanueva et al., 2017). The sampling design in the KK landscape with samples nested within 1 km landscapes units (Hernández-Stefanoni et al., 2011), resulting in short distances among sample plots within landscape units (minimum distance: 350 m) may have also contributed to this pattern of dominance by a few generalist species with wind-dispersed seeds, and to the small differences in species composition among successional age classes. In JMM, generalist species such as *Piscidia piscipula, Croton glabellus* and *Bursera simaruba* are also shared by early and intermediate successional classes, but very few of these remain as abundant as late-successional slow-growing species in old-growth forests (Table 3). These combined results suggest that species composition recovers quickly in the semi-deciduous forest of KK, but slowly in the semi-evergreen forest of JMM (Rozendaal et al., 2019). This interpretation is in agreement with the higher proportion of variation in species composition accounted for by successional age classes in JMM than in KK (Table 4) and with the greater ability of scores of NMDS axis 1 to separate successional age classes (especially the intermediate and old-growth ones) in JMM compared to KK (Fig. 7).

5. Conclusions

The methodological approach implemented in this study proved to be useful for producing accurate forest age maps in the two TDF landscapes studied. The segmentation processes of satellite images allowed us to better discriminate the area of interest based on high-resolution satellite images and chronosequence field data. Forest age maps are commonly obtained by means of time-series data that allow evaluating changes over time, using various types of medium-resolution satellite imagery. Our study showed that, by combining the spectral variability of high-resolution images with field data containing stand age information, it is possible to obtain highly accurate vegetation age maps for the TDF of the Yucatan Peninsula. The approach based on an initial segmentation followed by Random Forests classification proved to be effective for classifying high-resolution images. However, post-processing was key to attain a higher accuracy.

Forest age classes can be related to different vegetation attributes. Since successional age is strongly associated with forest structure, diversity and composition in the TDF studied (and in most forests worldwide), vegetation age classes can be related to various community attributes, such as above-ground biomass, species richness and species composition. However, our results show that the strength of the relationships varies between tropical dry forests, highlighting the importance of assessing these relationships separately for each forest type. Having accurate maps of vegetation age classes for each forest type is important for biodiversity conservation, forest management and restoration, land use planning and climate change mitigation strategies, such as REDD+ (reductions of emissions from deforestation and degradation and enhancement of carbon sequestration and other co-benefits). Having field data from forest stands of different ages since abandonment (i.e chronosequence data) in each forest type is key to adequately characterize secondary forest succession, which is essential to produce

accurate forest age maps and to relate age classes to vegetation attributes. This can help to better understand the resilience and the recovery of ecosystems after land use changes or natural disturbances, formulate strategies for sustainable management, biodiversity conservation, restoration and climate change mitigation.

Author contributions

Conceptualization and Methodology, GR-P and JLH-S. Writing-Original Draft Preparation, GR-P, JLH-S and JMD. Data Curation, GR-P and FJT-D. Investigation, GR-P and JLH-S. Writing-Review & Editing, GR-P, JMD, CAP_Q, JLA, FJT-D and JLH-S. Funding Acquisition, JLH-S. All authors have read and agreed to the published version of the manuscript.

Declaration of Competing Interest

The authors declare that they have no known competing financial interests or personal relationships that could have appeared to influence the work reported in this paper.

Acknowledgments

We thank James Callaghan and Kaxil Kiuic A. C. for providing logistic support. The study was financially supported by CICY and CONACYT FOMIX-Yucatán (project 108863). Finally, we want to thank María Elena Sánchez, who translated the first draft of the manuscript into English.

Appendix A. Supplementary data

Supplementary data to this article can be found online at https://doi.org/10.1016/j.ecolind.2020.106955.

References

Aguilar-Rodríguez, S., Abundiz-Bonilla, L., Barajas-Morales, J., 2001. Comparación de la gravedad específica y características anatómicas de la madera de dos comunidades vegetales en México. Anales del Instituto de Biología, Serie Botánica, p. 72.

Arroyo-Mora, J.P., Sánchez-Azofeifa, G.A., Kalacska, M.E., Rivard, B., Calvo-Alvarado, J. C., Janzen, D.H., 2005. Secondary forest detection in a Neotropical dry forest landscape using Landsat 7 ETM+ and IKONOS Imagery 1. Biotropica: J. Biol. Conserv. 37 (4), 497–507.

Avella, A., García, N., Fajardo-Gutiérrez, F., González-Melo, A., 2019. Patrones de sucesión secundaria en un bosque seco tropical interandino de Colombia. Caldasia 41 (1), 12–27.

Baccini, A., Goetz, S.J., Walker, W.S., Laporte, N.T., Sun, M., Sulla-Menashe, D., Hackler, J., Beck, P.S.A., Dubayah, R., Friedl, M.A., Samanta, S., Houghton, R.A., 2012. Estimated carbon dioxide emissions from tropical deforestation improved by carbon-density maps. Nat. Clim. Change 2 (3), 182.

Balvanera, P., Uriarte, M., Almeida-Leñero, L., Altesor, A., DeClerck, F., Gardner, T., Matos, D.M.S., 2012. Ecosystem services research in Latin America: the state of the art. Ecosyst. Serv. 2, 56–70.

Berberoglu, S., Lloyd, C.D., Atkinson, P.M., Curran, P.J., 2000. The integration of spectral and textural information using neural networks for land cover mapping in the Mediterranean. Comput. Geosci. 26 (4), 385–396.

Breiman, L., 2001. Random forests. Machine Learn. 45, 5–32.

Brown, S. (1997). Appendix 1—List of wood densities for tree species from tropical America, Africa, and Asia. Estimating biomass and biomass change of tropical forests: A primer. FAO Forestry Papers, 134.

Campbell, J.B., Wynne, R.H., 2011. Introduction to Remote Sensing. Guilford Press.

Cao, S., Yu, Q., Sanchez-Azofeifa, A., Feng, J., Rivard, B., Gu, Z., 2015. Mapping tropical dry forest succession using multiple criteria spectral mixture analysis. ISPRS J. Photogramm. Remote Sens. 109, 17–29.

Carreiras, J.M., Jones, J., Lucas, R., Gabriel, C., 2014. Land use and land cover change dynamics across the Brazilian Amazon: insights from extensive time-series analysis of remote sensing data. PLoS ONE 9 (8), e104144.

Carreiras, J.M., Jones, J., Lucas, R.M., Shimabukuro, Y.E., 2017. Mapping major land cover types and retrieving the age of secondary forests in the Brazilian Amazon by combining single-date optical and radar remote sensing data. Remote Sens. Environ. 194, 16–32.

Chazdon, R.L., 2003. Tropical forest recovery: legacies of human impact and natural disturbances. Perspect. Plant Ecol. Evol. System. 6 (1–2), 51–71.

Chazdon, R.L., 2014. Second Growth: The Promise of Tropical Forest Regeneration in an Age of Deforestation. University of Chicago Press.

Chazdon, R., Broadbent, E.N., Rozendaal, D.M.A., Bongers, F., Almeyda-Zambrano, A.M., Aide, T.M., Balvanera, P., Becknell, J., Boukili, V., Brancalion, P., Craven, D., Cabral, G., Jong, B., Denslow, J.S., Dent, D.H., Dewalt, S.J., Dupuy, J.M., Durán, S. M., Espirito-Santo, M.M., Fandino, M.C., Ricardo, G.C., Hall, J., Hernández-Stefanoni, J.L., Jacoyac, C., Junqueira, A., Kennard, D., Letcher, S.G., Lohbeck, M., Martínez-Ramos, M., Massoca, P., Meave, J., Mesquita, R., Mora, F., Muñoz, R., Muscarella, R., Nunes, Y., Ochoa-Gaona, S., Orihuela-Belmonte, E., Peña-Claros, M., Pérez-García, E., Piotto, D., Powers, J.S., Rodríguez, V., 2016. Carbon sequestration potential of second-growth forest regeneration in the Latin American tropics. Sci. Adv. 2, e1501639 https://doi.org/10.1126/sciadv.1501639.

Chave, J., Condit, R.S., Lao, S., Caspersen, J., Foster, R.B., Hubbell, S.P., 2003. Spatial and temporal variation of biomass in a tropical forest: Results from a large census plot in Panama. J. Ecol. 91, 240–252.

Chave, J., Andalo, C., Brown, S., Cairns, M.A., Chambers, J.Q., Eamus, D., Lescure, J.P., 2005. Tree allometry and improved estimation of carbon stocks and balance in tropical forests. Oecologia 145, 87–99.

Coelho, P.A., Santos, P.F., de Paiva, Paula E, Apgaua, D.M.G., Madeira, B.G., Menino, G. Cd.O., Nunes, Y.R.F., Santos, R.M., Tng, D.Y.P., 2016. Tree succession across a seasonally dry tropical forest and forest-savanna ecotone in northern Minas Gerais, Brazil. J. Plant Ecol. 2016 (10), 858–868.

Connell, J.H., 1978. Diversity in tropical rain forest and coral reefs. Science 199, 1302–1310.

Cutler A, Cutler DR and Stevens JR. 2012. "Random forests." Ensemble machine learning. Springer, Boston, MA, 2012. 157-175.

De la Barreda-Bautista, B., López-Caloca, A.A., Couturier, S., Silván-Cárdenas, J.L., 2011. Tropical dry forests in the global picture: the challenge of remote sensing-based change detection in tropical dry environments. Planet Earth 231–256.

Dorren, L.K., Maier, B., Seijmonsbergen, A.C., 2003. Improved Landsat-based forest mapping in steep mountainous terrain using object-based classification. For. Ecol. Manage. 183 (1–3), 31–46.

Dupuy, J.M., Hernández-Stefanoni, J.L., Hernández-Juárez, R.A., Tetetla-Rangel, E., López-Martínez, J.O., Leyequién-Abarca, E., May-Pat, F., 2012. Patterns and correlates of tropical dry forest structure and composition in a highly replicated chronosequence in Yucatan, Mexico. Biotropica 44, 151–162.

Eaton, J.M., Lawrence, D., 2009. Loss of carbon sequestration potential after several decades of shifting cultivation in the Southern Yucatán. For. Ecol. Manage. 258 (6), 949–958.

Fiorella M and Ripple WJ. 1995. Determining successional stage of temperate coniferous forests with Landsat satellite data.

Flores J and Espejel I. 1994. Etnoflora yucatanense, tipos de vegetación de la península de Yucatán. Universidad Autónoma de Yucatán. Mérida. Sostenibilidad Maya. pp. 73-80.

Frangi, J.L., Lugo, A.E., 1985. Ecosystem dynamics of a sub-tropical floodplain forest. Ecol. Monogr. 1985 (55), 351–369.

Frate, L., Carranza, M.L., Garfi, V., Febbraro, M.D., Tonti, D., Marchetti, M., Chirici, G., 2015. Spatially explicit estimation of forest age by integrating remotely sensed data and inverse yield modeling techniques. iForest-Biogeosci. Forest. 9 (1), 63.

Freeman EA, Frescino TS and Moisen GG. 2018. Model Map: an R package for model creation and map production. Web: https://cran. r-project. pdf Accessed, 10, 18.

Fujiki, S., Okada, K.I., Nishio, S., Kitayama, K., 2016. Estimation of the stand ages of tropical secondary forests after shifting cultivation based on the combination of WorldView-2 and time-series Landsat images. ISPRS J. Photogramm. Remote Sens. 119, 280–293.

Garcia Millan, V., Sanchez-Azofeifa, A., 2018. Quantifying changes on forest succession in a dry tropical forest using angular-hyperspectral remote sensing. Remote Sens. 10 (12), 1865.

Gallardo-Cruz, J.A., Meave, J.A., González, E.J., Lebrija-Trejos, E.E., Romero-Romero, M. A., Pérez-García, E.A., Martorell, C., 2012. Predicting tropical dry forest successional attributes from space: is the key hidden in image texture? PLoS ONE 7 (2).

González-Cruz, G., García-Frapolli, E., Casas, Fernández A., Dupuy Rada, J.M., 2015. Responding to disturbances: lessons from a Mayan social-ecological system. Int. J. Commons 9, 831–850.

Guyot J. 2011. Estimation du stock de carbone dans la végétation des zones humides de la Péninsule du Yucatan. Memoire de fin d'etudes. (Tesis de licenciatura no publicada). AgroParis Tech-El Colegio de la Frontera Sur.

Helmer, E.H., Ruzycki, T.S., Wunderle Jr, J.M., Vogesser, S., Ruefenacht, B., Kwit, C., Ewert, D.N., 2010. Mapping tropical dry forest height, foliage height profiles and disturbance type and age with a time series of cloud-cleared Landsat and ALI image mosaics to characterize avian habitat. Remote Sens. Environ. 114 (11), 2457–2473.

Hernández-Stefanoni, J.L., Dupuy, J.M., Johnson, K.D., Birdsey, R., Tun-Dzul, F., Peduzzi, A., López-Merlín, D., 2014. Improving species diversity and biomass estimates of tropical dry forests using airborne LiDAR. Remote Sens. 6 (6), 4741–4763.

Hernández-Stefanoni, J.L., Dupuy, J.M., Tun-Dzul, F., May-Pat, F., 2011. Influence of landscape structure and stand age on species density and biomass of a tropical dry forest across spatial scales. Landscape Ecol. 26 (3), 355–370.

Im, J., Jensen, J.R., Tullis, J.A., 2008. Object-based change detection using correlation image analysis and image segmentation. Int. J. Remote Sens. 29 (2), 399–423.

Karlson, M., Ostwald, M., Reese, H., Sanou, J., Tankoano, B., Mattsson, E., 2015. Mapping tree canopy cover and aboveground biomass in Sudano-Sahelian woodlands using Landsat 8 and random forest. Remote Sens. 7 (8), 10017–10041.

Le Quéré, C., Moriarty, R., Andrew, R.M., Canadell, J.G., Sitch, S., Korsbakken, J.I., Friedlingstein, P., Peters, G.P., Andres, R.J., Boden, T.A., Houghton, R.A., House, J.I., Keeling, R.F., Tans, P., Arneth, A., Bakker, D.C.E., Barbero, L., Bopp, L., Chang, J., Chevallier, F., Chini, L.P., Ciais, P., Fader, M., Feely, R.A., Gkritzalis, T., Harris, I., Hauck, J., Ilyina, T., Jain, A.K., Kato, E., Kitidis, V., Klein Goldewijk, K., Koven, C.,

Landschützer, P., Lauvset, S.K., Lefèvre, N., Lenton, A., Lima, I.D., Metzl, N., Millero, F., Munro, D.R., Murata, A., Nabel, J.E.M.S., Nakaoka, S., Nojiri, Y., O'Brien, K., Olsen, A., Ono, T., Pérez, F.F., Pfeil, B., Pierrot, D., Poulter, B., Rehder, G., Rödenbeck, C., Saito, S., Schuster, U., Schwinger, J., Séférian, R., Steinhoff, T., Stocker, B.D., Sutton, A.J., Takahashi, T., Tilbrook, B., van der Laan-Luijkx, I.T., van der Werf, G.R., van Heuven, S., Vandemark, D., Viovy, N., Wiltshire, A., Zaehle, S., Zeng, N., 2015. Global carbon budget 2015. Earth Syst. Sci. Data 7 (349–396), 2015. https://doi.org/10.5194/essd-7-349-2015.

Liu, D., Xia, F., 2010. Assessing object-based classification: advantages and limitations. Rem. Sens. Lett. 1 (4), 187–194.

Lillesand, T.M., Kiefer, R.W., 2004. Remote Sensing and Image Interpretation. JohnWiley and Sons, New York.

López-Jiménez, L.N., Durán-García, R., Dupuy-Rada, J.M., 2019. Recuperación de la estructura, diversidad y composición de una selva mediana subperennifolia en Yucatán, México. Madera y bosques 25 (1).

Lobo, A., Chic, O., Casterad, A., 1996. Classification of Mediterranean crops with multisensor data: per-pixel versus per-object statistics and image segmentation. Int. J. Remote Sens. 17 (12), 2385–2400.

Lucas, R.M., Honzak, M., Curran, P.J., Foody, G.M., Milne, R., Brown, T., Amaral, S., 2000. Mapping the regional extent of tropical forest regeneration stages in the Brazilian Legal Amazon using NOAA AVHRR data. Int. J. Remote Sens. 21, 2855–2881.

Magurran, A.E., 2004. Measuring Biological Diversity. Blackwell Publishing, Oxford.

Marin-Spiotta, E., Silver, W.L., Ostertag, R., 2007. Long-term patterns in tropical reforestation: Plant community composition and aboveground biomass accumulation. Ecol. Appl. 17 (3), 828–839.

Martínez-Ramos, M., Balvanera, P., Arreola Villa, F., Mora, F., Maass, J.M., Maza-Villalobos, S., 2018. Effects of long-term inter-annual rainfall variation on the dynamics of regenerative communities during the old-field succession of a neotropical dry forest. For. Ecol. Manage. 2018 (426), 91–100.

Maza-Villalobos, S., Balvanera, P., Martínez-Ramos, M., 2011. Early regeneration of tropical dry forest from abandoned pastures: contrasting chronosequence and dynamic approaches. Biotropica 43 (6), 666–675.

Miranda–Plaza EA. 2014. Factores que afectan la estructura de la vegetación en dos paisajes del bosque tropical seco de la Península de Yucatán. Tesis de Maestría. Centro de Investigación Científica de Yucata, CICY. Mérida, Yucatán, México.

Nelson, R.F., Kimes, D.S., Salas, W.A., Routhier, M., 2000. Secondary forest age and tropical forest biomass estimation using thematic mapper imagery: single-year tropical forest age classes, a surrogate for standing biomass, cannot be reliably identified using single-date tm imagery. Bioscience 50 (5), 419–431.

Oksanen J, Kindt R, Legendre P, O'Hara B, Stevens MHH., Oksanen MJ and Suggests MASS. 2007. The vegan package. Community ecology package, 10, 631-637.

Pasher, J., King, D.J., 2011. Development of a forest structural complexity index based on multispectral airborne remote sensing and topographic data. Can. J. For. Res. 41 (1), 44–58.

Poorter, L., Bongers, F., Aide, T.M., Almeyda Zambrano, A.M., Balvanera, P., Becknell, J. M., Bentos, T.V., Boukili, V.K., Broadbent, E.N., Chazdon, R.L., Craven, D., Cabral, G. A.L., de Almeida-Cortez, J.S., de Jong, B., Denslow, J.S., Dent, D.H., DeWalt, S.J., Dupuy, J.M., Durán, S.M., Espírito-Santo, M.M., Fandino, M.C., Hall, J.S., Hernández-Stefanoni, J.L., Jakovac, C.C., Junqueira, A.B., Kennard, D.K., Letcher, S. G., Lohbeck, M., Marín-Spiotta, E., Martínez-Ramos, M., Massoca, P.E.S., Meave, J. A., Mesquita, R.C.G., Mora, F., Muñoz, R., Muscarella, R., Nunes, Y.R.F., Ochoa-Gaona, S., Orihuela-Belmonte, E., Peña-Claros, M., Pérez-García, E.A., Piotto, D., Powers, J.S., Rodríguez-Velazquez, J., Romero-Pérez, I.E., Ruíz, J., Sanchez-Azofeifa, G.A., Swenson, N., Toledo, M., Uriarte, M., van Breugel, M., van der Wal, H., Veloso, M.D.M., Williamson, G.B., Rozendaal, D.M.A., 2016. Biomass resilience of Neotropical secondary forests. Nature 530 (7589), 211–214.

Portillo-Quintero, C., Sanchez-Azofeifa, A., Calvo-Alvarado, J., Quesada, M., Do Espirito Santo, M.M., 2015. The role of tropical dry forests for biodiversity, carbon and water conservation in the neotropics: lessons learned and opportunities for its sustainable management. Reg. Environ. Chang. 2015 (15), 1039–1049.

Portillo-Quintero, C.A., Sanchez-Azofeifa, G.A., 2010. Extent and conservation of tropical dry forests in the Americas. Biol. Conserv. 143, 144–155.

Powers, J.S., Feng, X., Sanchez-Azofeifa, A., Medvigy, D., 2018. Focus on tropical dry forest ecosystems and ecosystem services in the face of global change. Environ. Res. Lett. 13 (9), 090201.

QGIS Development Team. 2017. QGIS Geographic Information System. Open Source Geospatial Foundation Project. Available from http://qgis.org/en/site/.

R Development Core Team. 2017. R: A language and environment for statistical computing. R Foundation for Statistical Computing, Vienna, Austria. Disponible en: https://www.R-project.org/.

RColorBrewer, S., Liaw, M.A., 2018. Package 'randomForest'. University of California, Berkeley, Berkeley, CA, USA.

Ramírez Ramírez, G., Ramírez y Avilés, L., Solorio-Sánchez, F.J., Navarro-Alberto, J.A., Dupuy-Rada, J.M., 2019. Shifts in tree allometry in a tropical dry forest: implications for above-ground biomass estimation. Botan. Sci. 97 (2), 167–179. https://doi.org/10.17129/botsci.2101.

Reyes-García, C., Andrade, J.L., Simá, J.L., Us-Santamaría, R., Jackson, P.C., 2012. Sapwood to heartwood ratio affects whole-tree water use in dry forest legume and non-legume trees. Trees 26, 1317–1330.

Rozendaal D. M. A., N. Ascarrunz, F. Bongers, T. M. Aide, E. Alvarez-Dávila, P. H. S. Brancalion, P. Balvanera, J. M. Becknell, T. V. Bentos, R. G. César, G. A. L. Cabral, S. Calvo-Rodriguez, J. Chave, J. S. Almeida-Cortez, R. L. Chazdon, R. Condit, J. S. Dallinga, D. H. Dent, B. de Jong, A. de Oliveira, J. S. Denslow, M. M. Espírito-Santo, Saara J. DeWalt, J. M. Dupuy, S. M. Durán, L. P. Dutrieux, H. García, M. C. Fandino, G. W. Fernandes, B. Finegan, J. L. Hernández-Stefanoni, N. Gonzalez, V. Granda Moser, J. S. Hall, A. J. Hernández, S. Hubbell, C. C. Jakovac, S. G. Letcher, A. B. Junqueira, D. Kennard, D. Larpin, M. Martínez-Ramos, J. C. Licona, E. Lebrija-Trejos, E. Marín-Spiotta, P. E. S. Massoca, J. A. Meave, R. C. G. Mesquita, N. Norden, F. Mora, S. C. Müller, R. Muñoz, S. N. Oliveira Neto, R. Ostertag, Y. R. F. Nunes, S. Ochoa-Gaona, E. Ortiz-Malavassi, J. S. Powers, M. Peña-Claros, E. A. Pérez-García, D. Piotto, J. Rodríguez-Velázquez, J. Aguilar-Cano, S. Rodriguez-Buritica, A. Sanchez-Azofeifa, M. A. Romero-Romero, J. Ruíz, W. W. Thomas, A. Silva de Almeida, W. L. Silver, N. B. Schwartz, M. van Breugel, M. Toledo, M. Uriarte, E. V. S. Sampaio, M. D. M. Veloso, H. van der Wal, Sebastião Venâncio Martins, G. B. Williamson, H. F. M. Vester, A. Vicentini, I. C. G. Vieira, P. Villa, K. J. Zanini, J. Zimmerman, L. Poorter, 2019. Biodiversity recovery of Neotropical secondary forests. Science Advances 5: eaau3114. DOI: 10.1126/sciadv.aau3114.

Ruiz, J., Fandiño, M.C., Chazdon, R.L., 2005. Vegetation structure, composition, and species richness across a 56-year chronosequence of dry tropical forest on Providencia Island, Colombia 1. Biotropica: J. Biol. Conserv. 37 (4), 520–530.

Sanaphre-Villanueva, L., Dupuy, J.M., Andrade, J.L., Reyes-García, C., Paz, H., Jackson, P.C., 2016. Functional diversity of small and large trees along secondary succession in a tropical dry forest. Forests 7, 163.

Sanaphre-Villanueva, L., Dupuy, J.M., Andrade, J.L., Reyes-García, C., Jackson, P.C., Paz, H., 2017. Patterns of plant functional variation and specialization along secondary succession and topography in a tropical dry forest. Environ. Res. Lett. 12, 055004 https://doi.org/10.1088/1748-9326/aa6baa.

Song, D.X., Huang, C., Sexton, J.O., Channan, S., Feng, M., Townshend, J.R., 2015. Use of Landsat and Corona data for mapping forest cover change from the mid-1960s to 2000s: case studies from the Eastern United States and Central Brazil. ISPRS J. Photogramm. Remote Sens. 103, 81–92.

Stan, K., Sanchez-Azofeifa, A., 2019. Tropical dry forest diversity, climatic response, and resilience in a changing climate. Forests 10 (5), 443.

Sun, C., Cao, S., Sanchez-Azofeifa, G.A., 2019. Mapping tropical dry forest age using airborne waveform LiDAR and hyperspectral metrics. Int. J. Appl. Earth Obs. Geoinf. 83, 101908.

Torres, A.M., Adarve, J.B., Cárdenas, M., Vargas, J.A., Londoño, V., Rivera, K., Home, J., Duque, O.L., González, A.M., 2012. Dinámica sucesional de un fragmento de bosque seco tropical del Valle del Cauca. Colombia. Biota Colombiana 13 (2), 66–85.

White, D.A., Hood, C.S., 2004. Vegetation patterns and environmental gradients in tropical dry forests of the northern Yucatan Peninsula. J. Veg. Sci. 15 (2), 151–160.

van Rossum G. 1995. Python tutorial, Technical Report CS-R9526, Centrum voor Wiskunde en Informatica (CWI), Amsterdam.

Vieira, I.C.G., de Almeida, A.S., Davidson, E.A., Stone, T.A., de Carvalho, C.J.R., Guerrero, J.B., 2003. Classifying successional forests using Landsat spectral properties and ecological characteristics in eastern Amazonia. Remote Sens. Environ. 87 (4), 470–481.

Zhang, Y., Chen, H.Y., 2015. Individual size inequality links forest diversity and above-ground biomass. J. Ecol. 103 (5), 1245–1252.